Journal of Power Sources 191 (2009) 568–574

Contents lists available at ScienceDirect

Journal of Power Sources

journal homepage: www.elsevier.com/locate/jpowsour

Internal short circuit in Li-ion cells

Hossein Maleki*, Jason N. Howard

Motorola Inc Devices, 1700 Belle Meade Court, Lawrenceville, GA 30043, United States

ARTICLE INFO

Article history:
Received 7 January 2009
Received in revised form 20 February 2009
Accepted 23 February 2009
Available online 6 March 2009

Keywords:
Li-ion cells
Li-ion Batteries
Internal short circuit
Thermal stability

ABSTRACT

Effects of internal short circuit (ISCr) on thermal stability of Li-ion cells of various sizes (130–1100 mAh) are investigated using a combination of experimental methods and thermal modeling. Three experimental methods were evaluated: small nail penetration, small indentation, and cell pinch test. The small nail penetration and indentation tests created significant heat sinking to the cell-can or to the nail. Only the cell pinch test provided a reasonable approximation of a high risk ISCr event. ISCr location plays a critical role in the consequences of an ISCr event. ISCr at the edge of the electrode is the worst case because of its limited heat conduction to the cell-can. The effects of cell capacity and state of charge on ISCr are also evaluated through tests and thermal modeling.

1. Introduction

Portable electronic products, in particular cell-phones and laptop computers, demand for higher energy Li-ion batteries are increasing daily. Li-ion cell technology is now the primary source of energy for batteries used in most portable electronics because of its high energy density and long cycle-life. Li-ion cells consist of multiple layers of a carbon based material coated on copper foil (anode); lithium-metal oxides coated on aluminum foil (cathode); and a polymer membrane that electrically isolates the anode from the cathode (separator). A mixture of organic solvent and lithium-salt (electrolyte) provides an ionic conducting medium for the Li^+ ions to shuttle between the anode and the cathode during charge/discharge. The separator is made of a single-layer of polyethylene (PE) or tri-layers of polypropylene, polyethylene and polypropylene (PP/PE/PP).

Today's Li-ion cells are potentially vulnerable to abuse conditions; in particular, ISCr in $LiCoO_2$ based cells and/or charging to voltages above their recommended upper limits. Electrical abuse (overcharge and external short circuit) may be mitigated by control circuitry. Consequences of ISCr caused by mechanical abuse (drop, crush, etc.) or manufacturing issues will depend on the cell design, manufacturing quality, and nature of the event. While most ISCR events result in poor battery performance, in rare cases, ISCr can trigger thermal runaway. ISCr has been cited as the cause for field incidents and recalls of Li-ion batteries [1,2].

ISCr is an energetic process. Depending on cell design, up to 70% of the entire energy of the cell can be released in less than 60 s causing significant self-heating of the cell. During ISCr, the high electrical current (10–15 A) through the short circuited spot causes localized heating inside the cell. Risk of thermal runaway is then dependent on: (1) localized heating energy of the ISCr spot and its duration, (2) separator shrinkage, melting point and propagation, and (3) overall cell temperature rise.

Zhang et al. investigated various cell parameters and design cases affecting thermal performance of Li-ion cells during ISCr [1]. They suggest that Li-ion cells are at very high risk of thermal runaway if the uncoated section of the cathode Al-current collector contacts the anode surface. The anode heat propagation and solid electrolyte interface (SEI) layer thermal stability play critical roles in controlling the ISCr events in Li-ion cells. Barnet et al. investigated thermal performance of 2.2 Ah 18650 cells during ISCr [2] using modeling. They suggest that thermal energy of ISCr alone is sufficient to increase localized temperature of a cell by 200 °C. They also note that ISCr could cover a large percent of Li-ion battery field failures in portable electronics; although occurrence of thermal runway during ISCr is extremely rare. Application of high thermal stability materials and/or slowing down the active materials' thermal reactions is potential strategies to protect Li-ion cells from thermal runaway during ISCr. Horn suggests electrode material's uniformity could be the cause of soft-shorts in Li-ion cells [3]. Kawai notes the importance of lowering electrode-separator interfacial impedance in protecting Li-ion cells from thermal runaway during ISCr [4]. It has also been claimed that application of micro layers of ceramic coatings on the separator could mitigate the risk of thermal runaway during ISCr, especially for large Li-ion cells used in electric vehicle and hybrid electric vehicle applications

* Corresponding author.
E-mail address: HosseinMaleki@Motorola.con (H. Maleki).

0378-7753/$ – see front matter © 2009 Elsevier B.V. All rights reserved.
doi:10.1016/j.jpowsour.2009.02.070

Table 1
List of information on prismatic Li-ion cells internally short circuited (ISCr) using small-nail penetration.

Cell no.	Nominal size: $T \times W \times L$[a] (mm)	Cell mass (g)	Dischar. capacity (mAh)	Separator thickness (mm)	Anode thickness[b] (mm)	Cathode thickness[b] (mm)
1	5 × 34 × 50	21.1	1104	0.019	0.129	0.140
2	5 × 34 × 42	17.0	908	0.017	0.133	0.148
3	4 × 30 × 48	14.7	717	0.017	0.134	0.147
4	4 × 34 × 43	14.0	711	0.017	0.135	0.140
5	4 × 30 × 41	12.0	604	0.017	0.120	0.133
6	4 × 34 × 50	17.1	820	0.017	0.128	0.142

[a] T (thickness), W (width), and L (length).
[b] Anode and cathode thickness includes their materials coating pulse foils.

[5]. It has been suggested that the benefit is due to addition of the ceramic coating's strength and resistance to melting and shrinking of the separator. Furthermore, Li-ion battery manufacturers also test thermal stability of the cells prior to their products' assembly.

To date, various methods of testing thermal performance of Li-ion cells under ISCr have been proposed. However, it is difficult to create a small, isolated mechanical short circuit inside a finished cell that mimics the type of ISCr that may lead to a field incident. The common experimental methods that attempt to create an ISCr distort the overall cell integrity, create shorts in multiple locations, or sink heat and current to the cell can. Thus, analyzing ISCr's in finished Li-ion cells is limited by imperfect experimental methods.

In this work, we consider a combination of experimental and thermal modeling to evaluate testing methods and performance of Li-ion cells under ISCr, including:

1. Practicality of small nail penetration, cell indentation, and cell pinching used to simulate ISCr.
2. Effects of cell size and capacity on thermal performance of Li-ion cells during ISCr.
3. Effects of ISCr locations on thermal performance of Li-ion cells during ISCr.

2. Thermal Modeling of ISCr

The modeling is based on using a combination of measured electrical, electrochemical, and chemical heat generation of the cells during ISCr:

1- The electrical heat generation profile (Q_{Elect}) is obtained using current, voltage, and time values (Eq. (1)) from charged cells externally shorted circuited (ESCr) through a 1.0 mΩ resistor.
2- The electrochemical heat generation (Q_{Echem}) is obtained using the sum of the IR-drop, polarization, and the entropic heat effects of the cells (Eq. (2)). Charged cells were discharged at ISCr current using a current interruption method [6].
3- The chemical heat generation (QChem) of the ISCr location was determined using heat generation of charged cells measured by Accelerating Rate Calorimeter (ARC) [7]. The total heat generation of the cell is extrapolated to match the volume of the ISCr between two layers of cathode and anode.

$$Q_{Elect} = IV \tag{1}$$

$$Q_{Echem} = I(V_{ocv} - V_{op}) + IT\left(\frac{\Delta V}{\Delta T}\right) \tag{2}$$

$$Q_{Chem} = m\mathrm{Cp}\left(\frac{\Delta T}{\Delta t}\right) \tag{3}$$

$$Q_{Total} = Q_{Elect} + Q_{Echem} + Q_{Chem} \tag{4}$$

In Equations (1)–(3), the I and V are the cells' ESCr current (Amp) and voltage (V); the V_{ocv} and V_{op} are cells' rest and operation voltages; T is cells' temperature at which $\Delta V/\Delta T$ was measured using ARC; and m and Cp are the mass (g) and specific heat capacity (J g^{-1} °C) of the ISCr volume. The 1st and 2nd right hand terms in the Eq. (2) are known as irreversible (Q_{irrev}) and reversible (Q_{rev}) heats, respectively. Methods of measuring Cp and thermal conductivity (W/m °C) of cell components are described elsewhere [8].

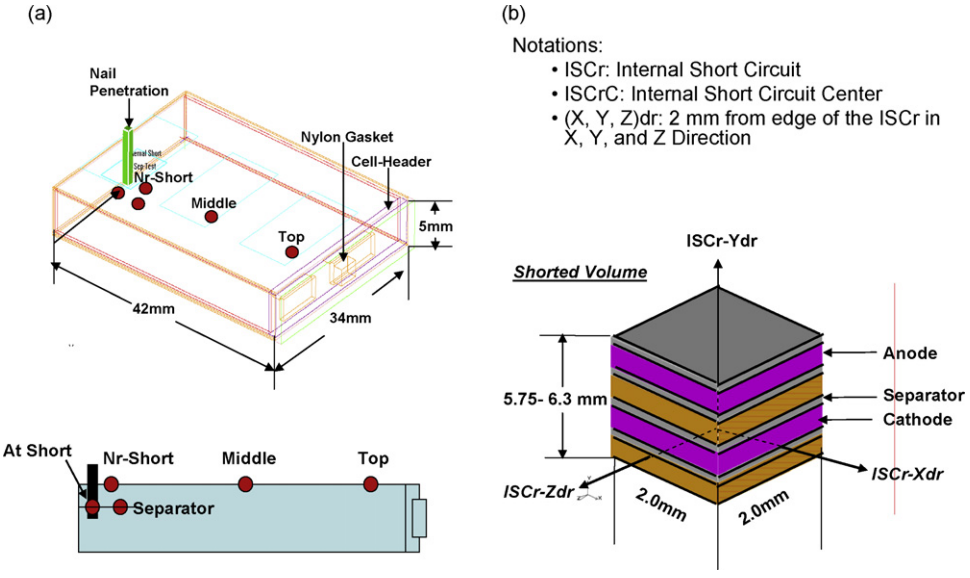

Fig. 1. Schematic of a prismatic cell under small-nail penetration test, (●) indicates where temperatures were monitored. (b) Schematic of internal short circuit volume used in thermal modeling of Li-ion cells: two layers of anodes, two layers of cathodes and four layers of separators. Notations—ISCr: internal short circuit; ISCrC: internal short circuit center (*X*, *Y*, *Z*) dr: 2 mm from edge of the ISCr in *X*, *Y*, and *Z* Direction.

In this modeling, both Q_{Elect} and Q_{Chem} are considered as heat sources for the ISCr volume, and the Q_{Echem} for the entire jelly-roll. The ISCr in itself causes localized heating of the cell initially, and soon after the electrochemical reactions take over due to the current flow through the electrode assembly before crossing the short circuited spot. This increases the entire cell temperature because of the cell internal impedance and high discharge current flow through the electrodes before reaching the ISCr spot.

3. Comparison of ISCr experimental simulation with thermal modeling

Several methods of testing ISCr response of Li-ion cells have been proposed. We compared experimental results from small-nail penetration (SNP), cell surface indentation (SIn), and cell pinching tests with thermal modeling. Table 1 lists information of the test cells' types, sizes, and capacity values. Cell samples were charged to the desired voltage at *C*-rate, and charging terminated when current dropped below 20 mA; For the Li-ion Polymer (LIP) cells, charging terminated when current dropped below 10 mA.

3.1. Small-nail penetration (SNP)

Fully charged cells (No. 1–6; Cap. 604–1104 mAh) were internally shorted by using a Brad-Nailer to insert a small nail (4.0 mm × 1.5 mm × 1.5 mm) 2–2.5 mm deep into the lower-middle section of each cell. Rubber based adhesive was applied at the nail penetration spot to minimize the cell electrolyte leakage during the test. Cell surface temperature was measured at three locations [Near (Nr) the Short, Middle, and Top]. The measurement continued until cell voltage dropped to near zero and temperature dropped after reaching a maximum. Comparable tests were simulated using thermal modeling. Fig. 1a shows a schematic of the SNP test and locations where the cells' temperatures were monitored. Fig. 1b shows a schematic of anode, cathode and separator layers arrangement (ISCr circuited volume) used in thermal modeling of cells during ISCr.

3.2. Surface indentation (SIn)

Two fully charged Li-ion polymer (LIP) cells (7 and 8; Capacity 350 and 130 mAh) were indented at the center of their largest surface using an arbor press with a special fixture. The fixture included a stainless-steel ball tip, sized to press 2.0–2.5 mm deep into the cells without puncturing their 0.22 mm thick outer nylon laminated aluminum foil cover. In this case, ISCr occurred while the separator ruptured and 2–3 layers of anodes and cathodes pressed into each other. Cell surface temperatures were measured at three locations (Nr-Short, Middle, and Top). Tests were continued until cell voltage dropped to near zero, and temperature dropped after reaching a maximum. Comparable tests were simulated using thermal modeling.

3.3. Modeling comparison with SNP and SIn

Fig. 2 compares both the SNP and the SIn experimental and modeling results showing reasonable agreements. Fig. 3 shows the thermal profile of cell-5 during SNP. Note that a large portion of heat from the ISCr location is transferred away from the ISCr spot by the nail itself. Fig. 4a–c are photos of separators recovered from cells 2, 3, and 5, respectively, after the SNP test. In these cases, separator melting propagation was limited to less than 4 mm wide, mainly because of fast cooling of the ISCr location due to heat transfer through the nail. Fig. 5 shows thermal profiles of cell-5 during SIn test. In this case, again, it is obvious that a large portion of the heat transferred to the cell-can because the ISCr is in contact with the

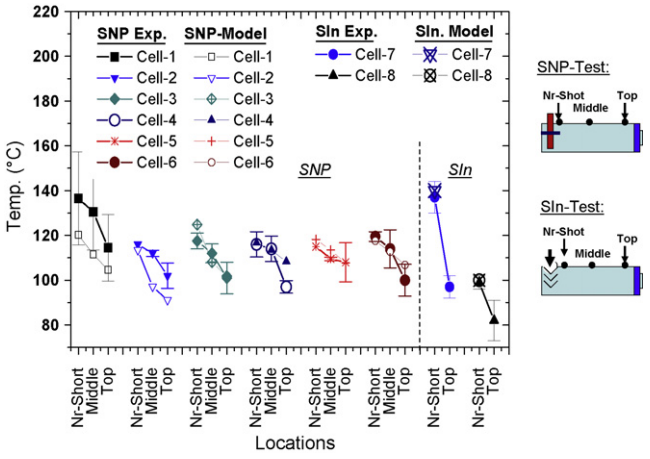

Fig. 2. Comparison of small-nail penetration (SNP) and small-indentation (SIn) testing and thermal modeling results. (●) locations where cell temperatures were monitored.

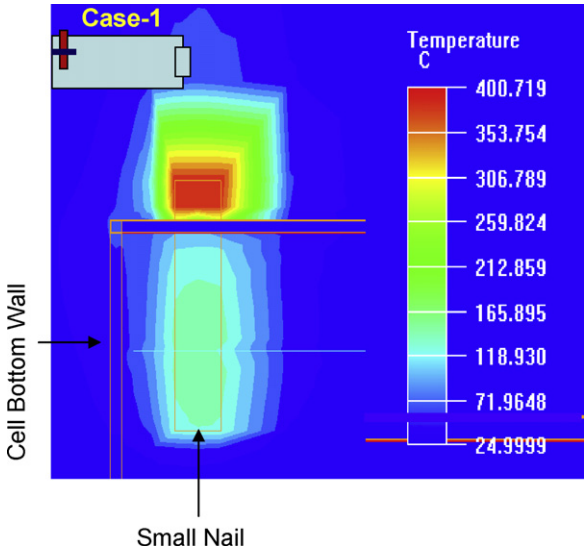

Fig. 3. Thermal modeling profiles of cell-5 under small-nail penetration test. The ISCr heat transfers through the nail to ambient surrounding the cell.

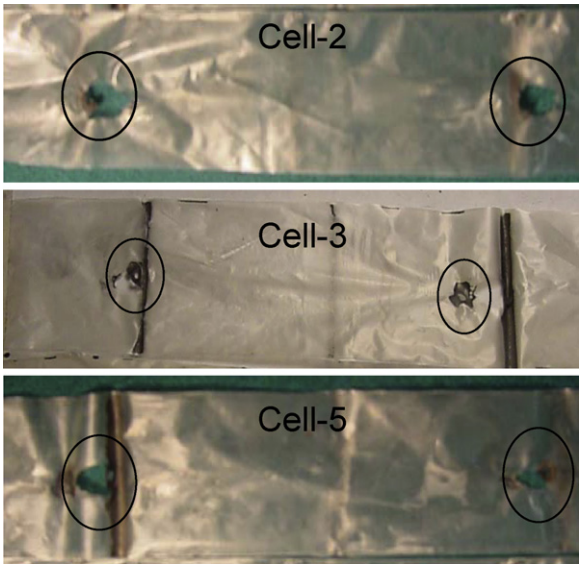

Fig. 4. Photos of separators recovered from cells 2, 3 and 5 after small-nail penetration test. Separator melting area circled.

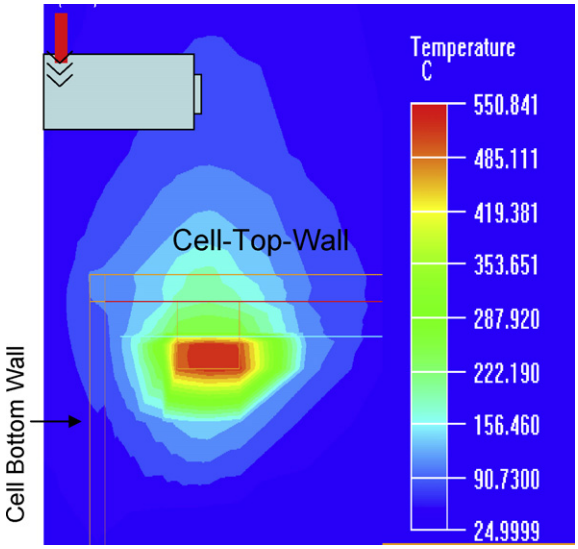

Fig. 5. Thermal modeling profile of cell-5 under Small-Indentation test. ISCr heat transfers to the cell-can.

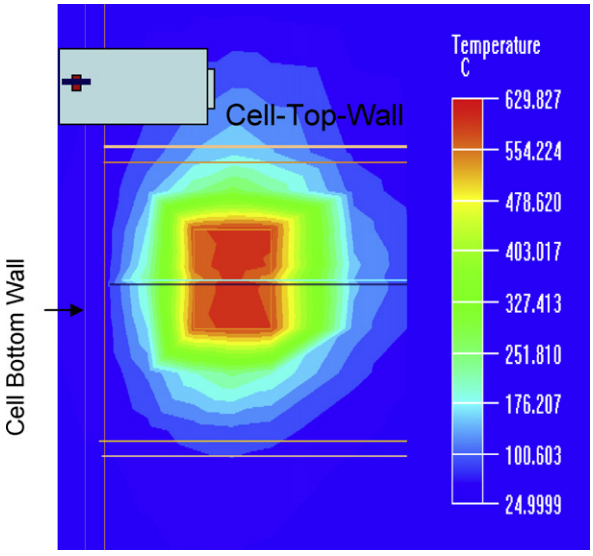

Fig. 6. Thermal modeling profile of cell-5. ISCr located among the two inner most layers of anode and cathode at the edge of the jelly-roll. ISCr heat is trapped inside the cell.

aluminum cell-can wall. Overall results suggest that the SNP or SIn tests do not mimic high risk ISCr events. Both tests create substantial heat sinking to the cell-can or the testing nail. Both situations reduce the likelihood of triggering thermal runaway.

Studies above support an understanding that thermal runaway from an ISCr event is more likely when there is a high rate of localized electrode heating with limited heat transfer to the cell-can. If the ISCr event occurs deep within the cell-winding structure, at a location with limited heat dissipation capability, the heat generation is initially localized; and then it must propagate through the cell jelly-roll before reaching the outer surface of the cell-can. This process increases cell internal temperature rise which ultimately affects the consequences of an ISCr event.

For confirmation, the thermal response of cell-5 was modeled with the ISCr located at the edges of the two inner most layers of anode and cathode facing the bottom of the cell-can. Fig. 6 shows the thermal profile of cell-5's modeled cross section. Note that the temperature of the cell and its ISCr location increases by 100–225 °C higher than those for SNP and SIn tests. Such results suggest a testing method that creates ISCr at edges of the inner most electrodes layers is a more realistic representation of a high-risk ISCR event than SNP and SIn tests.

3.4. Cell pinch-test

Further experiments showed that a cell-pinching test method produces ISCr events that are more similar to the high-risk events that could occur in the field. This method was used to evaluate cells of different sizes and capacities. The thin edge of a prismatic or

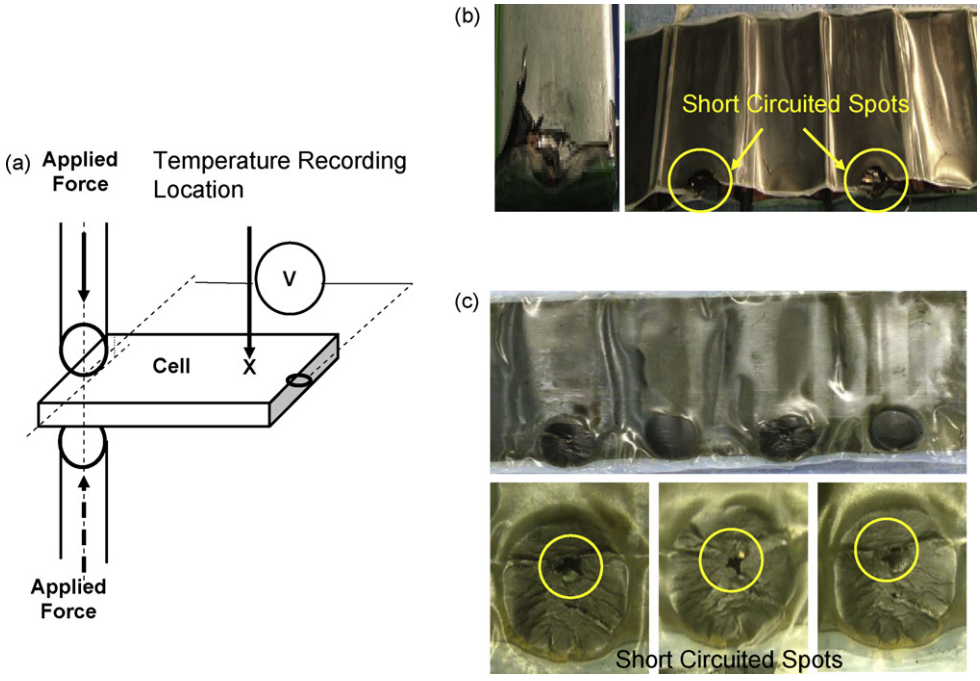

Fig. 7. (a) Schematic of Pinch-test setup. Cell edge is compressed by two opposite forces. Applied force stops once cell voltage falls to near 0.0 V. (b) Photos of jelly-roll and electrodes/separator assembly of a prismatic cell after Pinch-test. (c) Photos of electrodes/separator assembly of Li-ion polymer cell after Pinch-test.

Table 2
List and information on Li-ion polymer cells internally shorted circuited (ISCr) using Pinch-Test. Summary of test results also included. Cells with capacity higher than 260 mAh charged to 4.3 V or increased risks of thermal runaway during ISCr.

Cell no.	Size: $T \times W \times L$[a] (mm)	Cell mass (g)	Cells capacity (mAh)	Separator thickness (mm)	Anode thickness (mm)	Cathode thickness (mm)	No. of cells tested	Charged voltage (V)	Exp. maximum temperature (°C mean[b])	No. of cells ruptured and smoked
1	5 × 12 × 30	2.9–3.1	130	0.020	0.123	0.123	7 17 18	4.2 4.3 4.4	59 68 65	0 1 1
2	5 × 12 × 30	2.8–3.2	140	0.020	0.199	0.121	5	4.3	87	0
3	4 × 20 × 25	3.0–3.3	150	0.016	0.121	0.120	23 13	4.2 4.3	73 76	0 0
4	5 × 12 × 35	3.8–4.1	180	0.016	0.116	0.116	5	4.3	78	0
5	5 × 20 × 30	5.0–5.2	260	0.020	0.123	0.123	11 3	4.2 4.3	92 >150	1 2
6	5 × 27 × 30	6.7–7.1	350	0.1190	0.119	0.119	5	4.2	>400	4

[a] T (thickness), W (width), and L (length).
[b] Excluded cells that ruptured and smoked during Pinch-test.

polymer cell is compressed such that the 2–3 inner most layers of anode and cathode are pressed into each other. Fig. 7a shows a schematic of the test setup, and Fig. 7b and c are photos of a jelly-roll and electrodes recovered from charged prismatic and LIP cells after the pinch test. Pinch-testing has limitations in creating a highly reproducible ISCr condition, especially in the case of prismatic Li-ion cells with metallic cans. Therefore, thermal modeling is critical for a detailed understanding the behavior of Li-ion cells for different cases of ISCr (e.g. effects of ISCr location and/or capacity on risks of thermal runaway).

A combination of thermal modeling and cell pinch testing was used to study the thermal stability of Li-ion polymer (LIP) cells of different sizes and capacities at 4.2, 4.35 and 4.5 V. Table 2 provides the test cells' basic information and Pinch-Test results. Fig. 8 shows thermal modeling profiles of the ISCr spots and their surroundings with the maximum temperature set to 135 °C (melting point of PE based separator used in the cells). This setting predicts melting propagation of the separator surrounding the ISCr. Results show:

1. Temperature of the ISCr spot and its surroundings for the 132 mAh cell (charged to 4.2, 4.35 and 4.5 V) clearly remains below the melting point of the separator. Nearly similar conditions occur in the 140, 150 and 180 mAh cells charged to 4.2 and 4.35 V, and the 200 mAh cell charged to 4.2 V. Results suggest that heat generation of ISCr is not sufficient to cause separator melting propagation. Therefore, there is little chance of these cells going to thermal runaway under conditions described above.
2. For cells charged to 4.35 V and higher voltages, temperatures of the ISCr spots for both 200 and 260 mAh cells reach or exceed the melting point of the PE separator. Separator melting propagation is dependent on cell state of charge (SOC) and capacity, and these factors also increase the risk of thermal runaway during ISCr.

For confirmation we conducted pinch tests on some of the LIP cells charged to various SOC: 4.2 V covering batteries' normal operation, as well as 4.3 and 4.4 V covering limits for battery overcharge protection. Table 2 includes information on the LIP

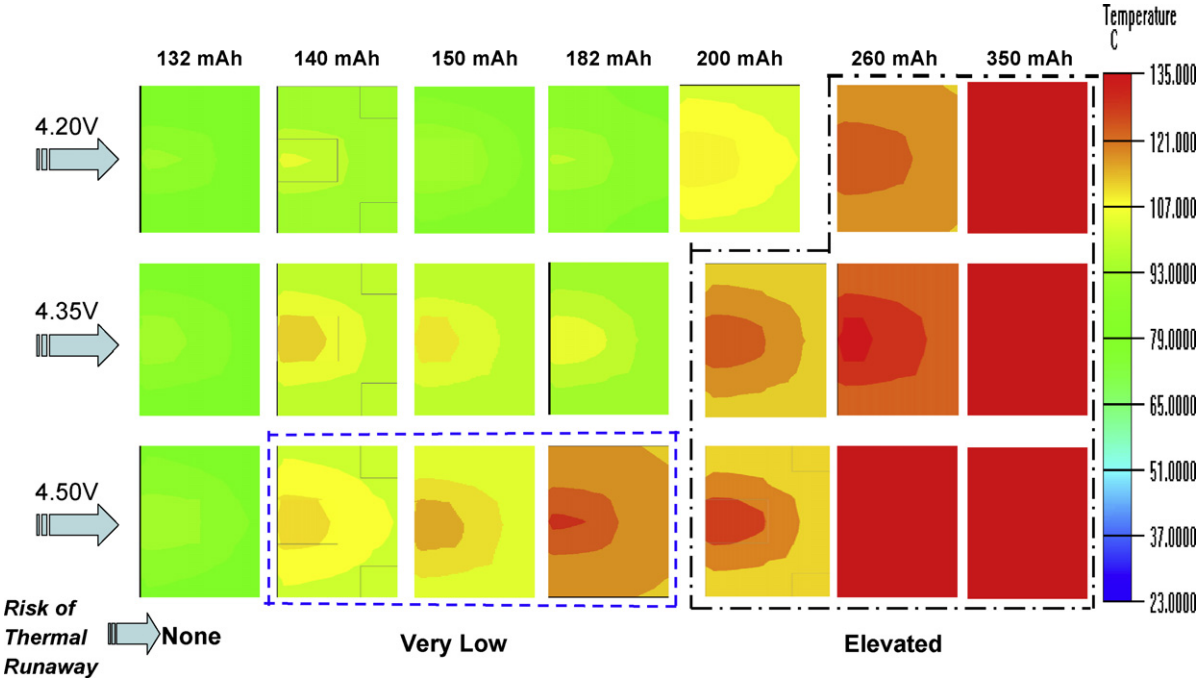

Fig. 8. Thermal profile of 4 mm × 4 mm separator surrounding the ISCr location. Maximum temperature is set at melting point of PE separator (135 °C) for clear resolution of temperature distribution.

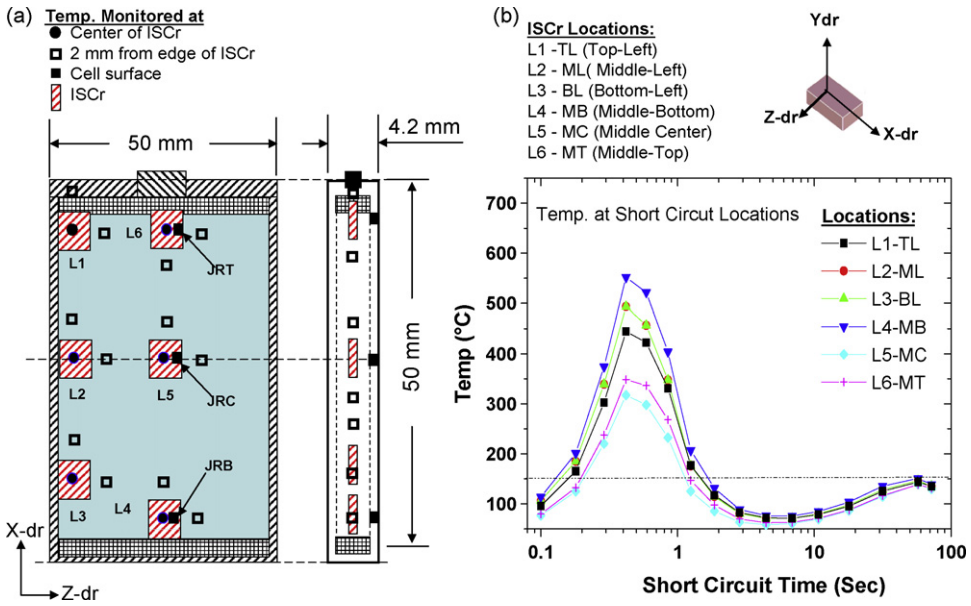

Fig. 9. (a) Schematic of the prismatic Li-ion cell (4 × 34 × 50) and the internal short circuit (ISCr) locations and their surrounding where cell temperatures were monitored. Individual models were run for each ISCr location. (b) superimposition of temperature vs. time profile for the ISCr location.

cells and their pinch test results that are in reasonable agreement with the modeling data. Both results show that LIP cells with capacity greater than 260 mAh are at risk of thermal runaway when charged to ≥4.2 V. Thermal response of the 200 mAh cell under ISCr could be marginal, while 130–180 mAh cells are not likely to reach thermal runaway, especially at voltages lower than 4.35 V.

4. Effect of ISCr Location

During our work we observed that thermal response of Li-ion cells changes depending on the ISCr location. Therefore, thermal modeling was used to investigate thermal response of a fully charged 790 mAh Li-ion prismatic cell (size: 4.2 mm × 34 mm × 50 mm) internally shorted at six different locations. The modeling is based on effects of the ISCr location on the temperature profile inside the cell.

Fig. 9a shows the ISCr locations (1–6) and their surroundings where the cell temperature was monitored. Fig. 9b shows a superimposition of temperature vs. time profiles for all the ISCr locations in the cell. Note that the temperature of the ISCr for location four (L4) reaches a higher temperature than that for all other cases. This is related to fact that the ISCr at L4 is near the jelly-roll bottom edge, however, the separator is 1 to 1.5 mm wider than the electrodes. Extra separator that fills the space between the jelly-roll edge and bottom section of the cell-can internal wall limits the heat transfer from ISCr to the cell-can. The low temperature case occurs at ISCr location five (L5) in the center of the cell. In this case, the heat is transferred in all directions surrounding the ISCr, facilitating heat dissipation. Therefore, location of the ISCr plays a role in the

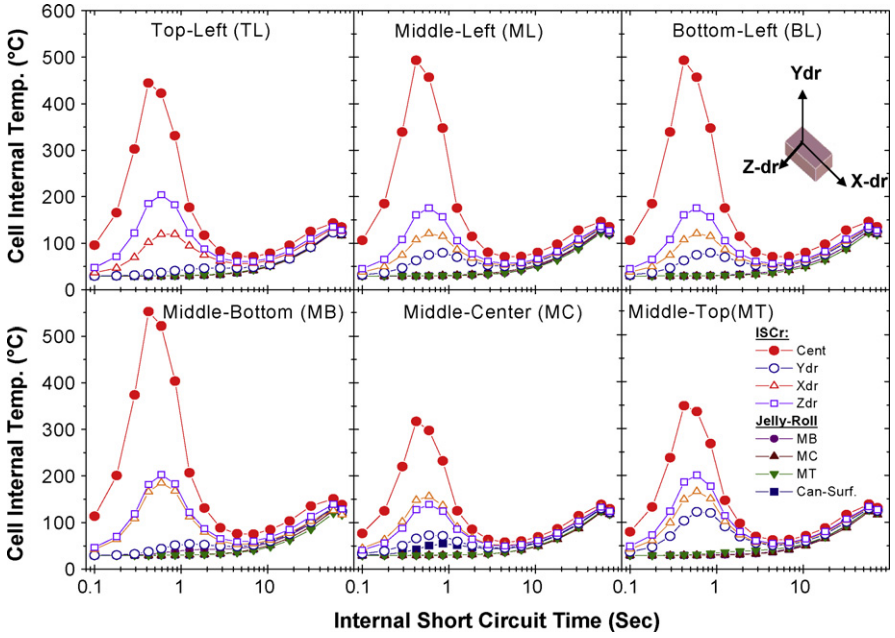

Fig. 10. Temperature vs. time profiles of internal short circuit (ISCr) and its surroundings at different locations inside of the prismatic (4 mm × 34 mm × 50 mm) cell.

thermal response of Li-ion cells during ISCr and will affect the risk of thermal runaway from an ISCr event.

Fig. 10 shows temperature vs. time profiles for each of the ISCr spots and their surroundings at the six different locations in the jelly-roll and for the cell outside surface. Note that the ISCr spot and its immediate surrounding reaches a maximum temperature (150–600 °C) in less than 1.0 s, followed by jelly-roll and cell surface temperature starting to increase 1.0–2.0 s after the beginning of the ISCr. After an immediate localized cooling of the ISCr hot spot, the cell overall temperature increases to 150–165 °C in 50–60 s, and finally the temperature of the entire cell starts cooling. Such temperatures cause separator melting and breakdown of the anode SEI-layer. Furthermore, 150–165 °C is within the range where the $LiCoO_2$ cathode plus electrolyte thermal decomposition reactions occur [9–12]. Combinations of such thermal events obviously increase the risk of thermal runaway during ISCr. High-risk ISCr events may occur when the ISCr is located where there is a gap between the electrode edges and the cell-can internal walls; or when the ISC heat generation is high enough to melt a large portion of separator. Pinch-test experimental results are consistent with this interpretation.

5. Conclusion

Combinations of experiments and thermal modeling were used to investigate test methods (Small Nail Penetration, Indention, and Pinch) simulating internal short circuits (ISCr) in prismatic Li-ion and Li-ion polymer (LIP) cells. Results indicated that pinching of the cell-edge where there are gaps between electrodes' edges and internal wall of the cell-can may create high risk ISCr events.

The risk of thermal runaway from ISCr events can increase with higher cell capacity, especially when the temperature of the ISCr and its surroundings exceed the separator melting point and approach the decomposition reaction temperature of cathode material with electrolyte. Among the cells tested, the LIP cells with 200 mAh or less capacity, charged to 4.35 V or less, have very low risk of reaching thermal runaway during ISCr. LIP cells with 260 mAh or higher capacity, charged to 4.2 V or higher, may have increased risk of going to thermal runaway during some types of ISCr events. Although the low capacity LIP cells can sometimes find application in small portable devices, they are not considered commercially practical for many electrical products that require higher electrical energy and/or power (for example mobile phones, notebook computers, and power tools).

ISCr location plays a critical role in the consequences of an ISCr event. ISCr at the edge of the electrode where the heat conduction to the cell-can is limited by low thermal conductivity of the electrolyte and separator materials (>0.3 W/m K) will have limited heat dissipation. Therefore, ISCr heat generation mainly transfers back into the jelly-roll through anode's copper and cathode's aluminum current collectors with high thermal conductivity.

Acknowledgements

Authors thank Russ Gyenes, Amy Herrmann and Jim Krause for technical advice. Special thanks to Corina Stanescu and Ed Louie for Pinch-Test experimental support.

References

[1] J. Zhang, S. Santhagopalan, P. Ramadass, IMLB-2008 Tianjin China, Abstract 74.
[2] B. Barnet, D. Ofer, B. Oh, R. Stringfellow, S. K. Singh, S. Sriramulu, J. IMLB-2008 Tianjin China, Abstract 75.
[3] Q. Horn, W. White, IMLB-2008 Tianjin China, Abstract 78.
[4] T. Kawai, ECS Conf., Fall 2006, Cancun Mexico.
[5] S. Augustin, V. Hennige, G. Horpel, C. Hying, J. Power Sources 146 (2003) 23–28.
[6] H. Maleki, A. Shamsuri, J. Power Sources 114 (2003) 131–136.
[7] H. Maleki, J. Howard, J. Power Sources 137 (2003) 117–127.
[8] H. Maleki, S. Al-Hallaj, R.J. Selmen, R. Dinwiddie, H. Wang, J. Electrochem. Soc. 146 (1999) 947–954.
[9] H. Maleki, G. Deng, A. Anani, J. Howard, J. Electrochem. Soc. 146 (1999) 3224–3229.
[10] D.D. MacNeil, J.R. Dahn, J. Electrochem. Soc. 148 (2001) 1205–1210.
[11] Z. Zhang, D. Fouchard, J.R. Rea, J. Power Sources 70 (1998) 16–20.
[12] E.P. Roth, D. H. Doughty, K. Amine, G. Henriksen, ECS Conf., (Fall 2003, Orlando FL.).